# Evaluation of DGT and DGT-PROFS modeling approach to estimate desorption kinetics of Cs in soils

Philippe Ciffroy, Loic Carasco, Daniel Orjollet, Caroline Simonucci, Laureline Fevrier

# Evaluation of DGT and DGT-PROFS modeling approach to estimate desorption kinetics of Cs in soils

Ciffroy P.[(1),*], Carasco L.[(2)], Orjollet D.[(2)], Simonucci C.[(3),(4)] and Février L.[(2),*]

[(1)] EDF, Division Recherche et Développement, Laboratoire National d'Hydraulique et Environnement, 6 quai Watier, 78401 Chatou, France

[(2)] Institut de Radioprotection et de Sûreté Nucléaire (IRSN), PRP-ENV, SRTE, LR2T, Cadarache, France

[(3)] Institut de Radioprotection et de Sûreté Nucléaire (IRSN), PRP-ENV, SEDRE, LELI, Fontenay-aux-Roses, France

[(4)] Present address: Institut de Radioprotection et de Sûreté Nucléaire (IRSN), PRP-ENV, SIRSE, LERNORD, Fontenay-aux-Roses, France

*Corresponding author: philippe.ciffroy@edf.fr; laureline.fevrier@irsn.fr

**Accepted in Journal of Environmental Radioactivity**

https://doi.org/10.1016/j.jenvrad.2021.106646

## Abstract

The aim of this paper is to assess the suitability of DGT to extract kinetic rates of desorption of cesium (Cs) from soils. For this purpose, laboratory experiments with a natural soil spiked with Cs were carried out under three different contamination conditions, reflecting either an increase in Cs contamination level or an ageing of the contamination within the soil. The experimental results, i.e. the Cs accumulation kinetics onto DGT probes were interpreted by the DGT-PROFS model. The latter calculates the partitioning of Cs between two particulate pools, describing weak and strong interactions respectively, as well as kinetic rates describing exchange reactions. Experimental conditions did not show any major impact on desorption rates, suggesting that desorption kinetics were not significantly affected by contamination level and ageing. Instead, the distribution of Cs among

weak and strong sites was shown to be the predominant factor governing the differences observed in the remobilization of Cs to porewater among experimental conditions. The DGT technique combined with the DGT-PROFS modelling approach was proved to be efficient in estimating desorption kinetic rates of Cs in soils.

## 1. Introduction

$^{137}$Cs is an important fission product of the irradiation of uranium-based fuels. It is one of the most released radionuclides in the environment due to nuclear weapons testing or nuclear accidents, going from leakage from high level waste storage sites such as Hanford, USA (Zachara et al., 2002) or Mayak, Russia (Balonov et al., 2007) to large environmental spreading after Chernobyl or Fukushima accidents (Steinhauser et al., 2015; Beresford et al., 2016). Once released into the environment, $^{137}$Cs penetrates the soil. Due to its chemical similarity with K, it can then be taken up by plants and enter the human food chain. Because of its high radioactivity and relative long half-life ($t_{1/2}$ = 30 years), it represents a hazard for human health due both to internal contamination through food-chain and external exposure to gamma-ray. Therefore understanding its behaviour and predicting its mobility in the terrestrial environment is still of major importance.

In soils (or sediments), Cs interacts mainly with clay minerals, which contain highly selective sorption sites for alkali metals such as Cs and K (Evans et al., 1983; Cremers et al., 1988). Sorption of Cs on clay minerals involve multiple sites (including planar surface sites, edge sites, hydrated interlayer sites, frayed edge sites – FES - and interlayer sites) exhibiting different affinities and specificities for Cs (Okumura et al., 2018). The highest binding sites in terms of affinity, which are also the lowest in terms of density, are the so-called FES located at the wedge-shaped edges of micaceous clay minerals, particularly on illite. The involvement of sorption sites exhibiting different Cs capacities and affinities result in a non-linear sorption of Cs in soils as function of Cs concentration. Classical S-shape sorption isotherms are usually found; which means that the solid-liquid distribution of Cs depends on the concentration of Cs (Missana et al., 2014). Macroscopically, sorption of Cs on clay minerals (Brouwer et al., 1983; Poinssot et al., 1999; Bradbury and Bayens, 2000; Cherif et al., 2017; Siroux et al., 2018) but also onto complex phases (Cherif et al., 2017; Siroux et al., 2018; Wissocq et al., 2018), in soils (Missana et al., 2014) or in sediments (Fuller et al., 2014) has been successfully described by thermodynamic models assuming either surface complexation and/or ion exchange on reactive sites, two or three reactive sites, and an additivity of the reactive components.

If sorption of Cs on montmorillonite and kaolinite is expected to be reversible, sorption/desorption experiments highlighted an apparent irreversibility of Cs sorption on illite (Comans et al., 1991; Comans and Hockley, 1992). This behaviour has been interpreted as the result of the collapse of hydrated interlayers of illite in which the Cs was trapped or of the slow migration of Cs into core region of illite particles (Comans and Hockley, 1992; De Koning and Comans, 2004; Okumura et al., 2018). Recently Durrant et al. (2018) showed that desorption of Cs from illite is in fact totally reversible, at least for concentration of Cs in solution below $10^{-5}$M. However the amount desorbed is very low due to the high values of affinity constants between Cs and illite. Besides, the outcome of the slow migration of Cs into core region of illite particles is that increased contact time between Cs and particles - or in other term the ageing of contamination - may decrease the amount of readily extractable Cs from illite (Fuller et al., 2015; Durrant et al., 2018; Okumura et al., 2018).

In addition to clay minerals, organic matter is another potential sorbent of Cs in soils. However, its role is still debatable and seems to depend on its content in soils. In soils with high organic matter content (>80%), it has been shown to play a significant role in Cs sorption (Valcke and Cremers, 1994; Rigol et al., 2002; Lofts et al., 2002). However, on soil containing less than 40 % of organic matter, Valcke and Cremers (1994) showed that the clays FES are the main sorption sites for Cs. Moreover, no data regarding the reversibility of Cs sorption on soil organic matter has been reported.

As a result, modelling the desorption dynamics of Cs in soils and sediments requires the description of at least two particulate pools with different interaction strengths and kinetics (Absalom et al., 1996; Ciffroy et al., 2003; Garnier et al., 2006; Murota et al., 2016). Only a very small pool of Cs is considered as readily desorbable (Kasar et al., 2020). The other pools are either considered as irreversibly fixed or following a very slow kinetic rate of desorption. As for clay minerals, ageing increased the stability of Cs sorption in soils and sediments and reduces the amount readily desorbable (Valcke and Cremers, 1994; Rigol et al., 1999a; Ciffroy et al., 2001; Al Attar et al., 2016; Tachi et al., 2020). Since Cs persists in the environment, quantifying the amount and rate of Cs release from soils is still of major importance to predict correctly the gradual migration of Cs in deeper soil horizons or the amount available for uptake by plants at long time scale (Murota et al., 2016; Brimo et al., 2019; Chaif et al., 2021).

Information on trace metals (TMs) exchange between soil particles and soil solution has already been assessed by using the diffusive gradient in thin-films (DGT) technique, which is a dynamic *in situ* sampling technique of labile TMs in solution (Zhang et al., 1998). The principle behind DGT is that the sampler provides a localized region of low metal concentration, which promotes a diffusive flux of TM into the sampler. Interpretation of TM fluxes into the DGT sampler indicates the degree of depletion of the metal concentration at the device interface, the kinetics of desorption of the metal, and the size

of the pool(s) of labile metal in the particulate phase. Interpretation of DGT measurements in soils requires a conceptual model of TMs sorption/desorption reactions and diffusion in soils (Cornu et al., 2007) as well as a numerical model for fitting geochemical parameters of concern. For this purpose, Harper et al. (1998) and Sochaczewski et al. (2007) developed the 'DGT-Induced Fluxes in Soils and Sediments' models (1D-DIFS and 2D-DIFS), which allow calculating the distribution ratio $K_{dl}$ between fractions of TM respectively adsorbed on particles and dissolved in solution, and the response time $T_c$, which describes metal resupply kinetics from the solid phase. Despite their undisputable performance and wide dissemination among DGT users, the DIFS models showed flaws in some cases. Firstly, the DIFS model considers a single pool of labile adsorbed TM. Yet, it was shown that a single pair of forward and reverse rate constants is sometimes inaccurate and that multiple types of sorption sites should instead be used for describing multiple-stage kinetics (Ernstberger et al., 2002; Lehto et al., 2008; Nowack et al., 2004; Cornu et al., 2007; Mihalik et al., 2012). Secondly, it was shown in some cases that a number of combinations of $K_{dl}$ and $T_c$ can be fitted to an experimental data set with equivalent results (Lehto et al., 2008). To overcome such limitations, Ciffroy et al. (2011) developed the DGT-PROFS model. This model considers the soil (or sediment) as having two labile solid phases instead of one and advanced methods for probabilistic and sensitivity analysis, allowing us to represent parameters by Probability Distribution Functions (PDFs) instead of best estimates. These models are able to quantify TM partitioning between the pools they consider (Nia et al., 2011). In the case of DGT-PROFS model, the partitioning between two particulate pools, describing weak and strong interactions with TM, is thus calculated.

DGT was originally developed for divalent cations and its adaptation for other elements requires the development of specific resins. This explains limited applications of DGT for sampling Cs in natural environments (Chang et al., 1998; Murdock et al., 2001; Li et al., 2009; Gorny et al., 2019). In the time-restricted framework of the NEEDS-Environment funded projects, we therefore proposed to assess the ability of the DGT technique to be used to extract information on Cs desorption dynamics in soils. A set of kinetics laboratory experiments with a natural soil spiked with Cs was performed. The DGT-PROFS model was used to interpret the measurement and give insight into Cs desorption kinetic parameters. Regarding Cs sorption features described above, a special attention was given to the effects of Cs concentration and Cs contamination ageing on the desorption behaviour of Cs in soils.

## 2. Material and methods

### 2.1 Preparation of Cs-specific DGT

The DGT technique is described in detail in other papers (e.g. Davison and Zhang, 1994). Then, only the design of specific DGT samplers for Cs is described here.

AMP (Ammonium Molybdo Phosphate, $2PO_4(NH_4)_3 24MoO_3,3H_20$) was selected as a reliable chelating gel material for sampling radiocesium (Murdock et al., 2001; Gorny et al., 2019). The chelating gels were acrylamide hydrogels, made using AMP, acrylamide monomer, ammonium persulfate initiator and TEMED catalyst according to the procedure described in Gorny et al. (2019). Diffusive gels were standard diffusive gel discs in agarose crosslinked polyacrylamide (APA) purchased from DGT Research Ltd. (Lancaster, UK); with a thickness of 0.78 mm. The gel was assembled in a standard plastic DGT holder with a window area of 2.54 $cm^2$. A membrane filter with a 0.40 µm porosity (IsoporeTM Membrane Polycarbonate Filters) extended the DGT diffusive layer thickness by 0.13 mm and protected the gel from particles.

### 2.2 Soil spiking and deployment of DGT in soils

Soil used for the experiments was sampled at Auzeville (Haute Garonne, France) over a depth of 10 cm and was previously characterized by Devau et al. (2011). It was dried and sieved at 2 mm. The organic carbon concentration was measured by heat-loss weight at 1000 °C whereas the cation exchange capacity (CEC) and the concentrations of the exchangeable cations were determined by extraction with cobalthexamine chloride. Its main physico-chemical characteristics are reported in Table 1. From a textural point of view, it is a silty-clay soil (with a clay content > 35%). Among clay minerals, illite and kaolinite are the predominant ones (content around 10%), whereras montmorillonite content is about 4% of soil fraction below 2mm. This soil has a rather low organic carbon content, with a rate not exceeding 1%. Measurement of natural stable Cs background in this soil was not performed, since Cs from background was not expected to be mobile and to interfere in the experiments.

337 **Table 1** - Physico-chemical characteristics of the soil used for the experiments
338

| | |
|---|---|
| pH | 6.53 |
| Organic carbon (g.kg$^{-1}$ dry weight) | 9.82 |
| CEC (cmol. kg$^{-1}$ dry weight) | 11.52 |
| Ca (cmol. kg$^{-1}$ dry weight) | 9.31 |
| Mg (cmol. kg$^{-1}$ dry weight) | 1.22 |
| Na (cmol. kg$^{-1}$ dry weight) | 0.05 |
| K (cmol. kg$^{-1}$ dry weight) | 0.71 |
| Illite (g.kg$^{-1}$ dry weight) | 100 |
| Montmorillonite (g.kg$^{-1}$ dry weight) | 39 |
| Kaolinite (g.kg$^{-1}$ dry weight) | 101 |
| Goethite (g.kg$^{-1}$ dry weight) | 4.9 |

339

340 Three spiking conditions were defined for generating contrasted contaminated soils. For each of these
341 three conditions, 290 g dry weight of soil were spiked with a solution containing known and predefined
342 quantities of stable cesium ($^{133}$Cs) and radiocesium ($^{137}$Cs). $^{137}$Cs, which is naturally not present in this
343 soil, was used to trace the behavior of freshly added Cs. The three conditions, hereafter noted
344 conditions A, B, and C respectively, correspond to soils contaminated with the following levels:

345 • Condition A: 1.18.10$^{-7}$ mol.g$^{-1}$ dry weight of total Cs ($^{133}$Cs and $^{137}$Cs) and 1.93.10$^{3}$ Bq.g$^{-1}$ dry
346 weight of $^{137}$Cs. The contaminated soil was used within three days after spiking;
347 • Condition B: 1.09.10$^{-5}$ mol.g$^{-1}$ dry weight of total Cs ($^{133}$Cs and $^{137}$Cs) and 1.94.10$^{3}$ Bq.g$^{-1}$ dry
348 weight of $^{137}$Cs. The contaminated soil was used within three days after spiking;
349 • Condition C: 1.09.10$^{-5}$ mol.g$^{-1}$ dry weight of total Cs ($^{133}$Cs and $^{137}$Cs) and 1.94.10$^{3}$ Bq.g$^{-1}$ dry
350 weight of $^{137}$Cs. The contaminated soil was stored during 3 months prior DGT kinetic
351 experiments for studying the ageing effect.

352 After spiking procedure and equilibration period, contaminated soils were distributed in equal
353 quantities (15 g dry weight) to plastic beakers with a diameter of 4.3 cm, representing soil depth
354 ranging from 1 to 1.5 cm. Quantities of soils have been chosen to obtain a soil layer thickness higher
355 than the DGT probe influence depth. The soil samples were then moistened until a fine water layer
356 formed at the soil surface and incubated for one hour before DGT probes were deployed. Final
357 gravimetric water content (mass water/mass dry soil) was about 48%.

358

## 2.3 Kinetic experiments and $^{137}Cs$ analyses

After the equilibration period, DGT devices were gently pressed into the soil until the filter of the device was in contact with the surface of the soil housing. The experimental units were then closed and incubated at constant temperature (20°C) in the dark in a thermostated chamber (Figure 1). The water content was kept constant during the whole incubation. The DGT devices were then removed from the soils at different contact times, i.e 4, 8, 16, 24 and 96 hours. Three replicates were analyzed for each condition and at each time point (noted X1, X2 and X3 hereafter). At time 4 and 96 hours, the porewater was extracted from 2.5 g of soil by centrifugation at 20 000 g for one hour. The volume of extracted porewater ranged between 200 and 450 µl. $^{137}Cs$ was analyzed by gamma-spectroscopy after acidification (using a pure germanium gamma spectrometer – Camberra). Quantity detected were always above the detection limit of the method.

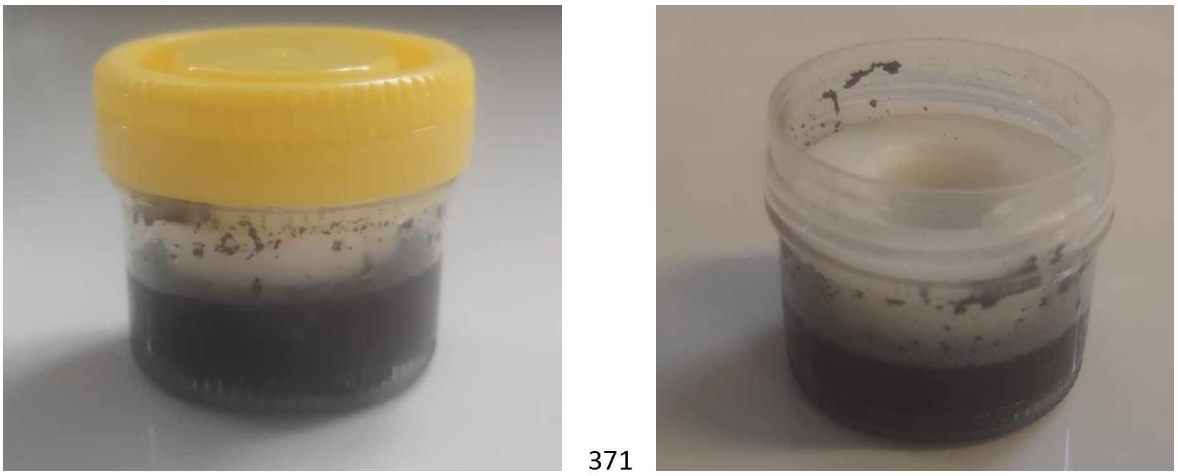

**Figure 1** – Experimental device

After deployment, the DGT probes were retrieved and jet-washed with deionized water to remove soil particles before being disassembled. $^{137}Cs$ was analyzed directly on the chelating gel by gamma spectroscopy as described in Murdock et al. (2001).

## 2.4 DGT-PROFS modeling approach

The accumulation kinetics of Cs to DGT were interpreted by the DGT-PROFS model thoroughly described in Ciffroy et al. (2011). The model is coded with the Ecolego® tool (https://www.ecolego.se/). Briefly, the model considers that transport in both the diffusion layer (DGT gel) and soil porewater is solely driven by molecular diffusion and that all labile Cs species in porewater have a single self-diffusion coefficient. It is a one dimensional model operating along the axis perpendicular to the DGT interface. These assumptions are strictly the same as those considered by Harper et al. (1998) and

384 Harper et al. (2000) for the 1D-DIFS model. Unlike the DIFS model described in Harper et al. (1998), the
385 DGT-PROFS model assumes that Cs in soil can be distributed between three separate phases: (i)
386 porewater (where speciation may influence the diffusion coefficient values in soil solution and in DGT
387 gel), (ii) weak and (iii) strong sorption sites on the particulate phase. This model assumes that
388 interactions with weak and strong sites can be described by consecutive reactions (reactions 1 and 2):

389 (Reaction 1) $$M_{pw,labile} + S_{weak} \underset{k_{des,1}}{\overset{k_{ads,1}}{\rightleftharpoons}} MS_{weak}$$

390 (Reaction 2) $$MS_{weak} + S_{strong} \underset{k_{des,2}}{\overset{k_{ads,2}}{\rightleftharpoons}} MS_{strong} + S_{weak}$$

391 where $M_{pw,labile}$ is labile Cs in the porewater (mol.cm$^{-3}$); $S_{weak}$ and $S_{strong}$ are particles weak and
392 strong sites respectively (mol.g$^{-1}$); $MS_{weak}$ and $MS_{strong}$ are the concentration of Cs on the weak and
393 strong particulate sites respectively (mol.g$^{-1}$); and $k_{ads,1}$, $k_{des,1}$, $k_{ads,2}$, $k_{des,2}$ are sorption-desorption
394 rate constants on or from the weak and strong sites (g.mol$^{-1}$.s$^{-1}$; s$^{-1}$; g.mol$^{-1}$.s$^{-1}$; g.mol$^{-1}$.s$^{-1}$, respectively).

395 To simplify the equations, the conditional rate constants $k^*_{ads,1}$ $k^*_{ads,2}$ and $k^*_{des,2}$ (s$^{-1}$) are defined
396 depending on concentrations of the weak and strong available sites $(S_{weak})$ and $\left(S_{strong}\right)$ as follows:

397 (Equation 1) $$k^*_{ads,1} = k_{ads,1}.\,(S_{weak})$$

398 (Equation 2) $$k^*_{ads,2} = k_{ads,2}.\left(S_{strong}\right)$$

399 (Equation 3) $$k^*_{des,1} = k_{des,1}$$

400 (Equation 4) $$k^*_{des,2} = k_{des,2}.\,(S_{weak})$$

401 The distribution of Cs between weak and strong sorption sites is described by $\alpha_{weak}$, which indicates
402 the proportion of Cs adsorbed onto the weak sites before DGT deployment:

403 (Equation 5) $$\alpha_{weak} = \frac{(MS_{weak})_{t=0}}{(MS_{weak})_{t=0} + \left(MS_{strong}\right)_{t=0}}$$

404 The accumulation of Cs on DGT is governed by the adsorption-desorption kinetics described in
405 reactions 1 and 2, and by the diffusion of Cs within soil porewater and DGT gel. Diffusion in soil and
406 chemical reactions lead to the following set of mass-balance equations:

407 (Equation 6) $$\frac{\partial(M_{pw,labile})}{\partial t} = D_{sed}.\frac{\partial^2(M_{pw,labile})}{\partial x^2} - k^*_{ads,1}.\left(M_{pw,labile}\right) + k^*_{des,1}.Sed.\,(MS_{weak})$$

408 (Equation 7) $$\frac{\partial(MS_{weak})}{\partial t} = \frac{k^*_{ads,1}.(M_{pw,labile})}{Sed} - \left(k^*_{des,1} + k^*_{ads,2}\right)(MS_{weak}) + k^*_{des,2}\left(MS_{strong}\right)$$

409 (Equation 8) $$\frac{\partial(MS_{strong})}{\partial t} = k^*_{ads,2}(MS_{weak}) - k^*_{des,2}.\left(MS_{strong}\right)$$

where $D_{sed}$ is the apparent diffusion coefficient of Cs in soil ($cm^2.s^{-1}$) and $Sed$ is the concentration of particles in soil ($g.cm^{-3}$).

Only labile Cs, $M_{pw,labile}$, (i.e., free Cs and small inorganic complexes able to dissociate in the gel) are assumed to diffuse in the DGT gel, with only one kinetic equation describing transport in the diffusive layer of the DGT device:

(Equation 9) $$\frac{\partial(M_{pw,labile})}{\partial t} = D_{gel}.\frac{\partial^2(M_{pw,labile})}{\partial x^2}$$

where $D_{gel}$ is the apparent diffusion coefficient of Cs in the DGT gel ($cm^2.s^{-1}$).

In the specific case of Cs however, speciation in soil porewater (e.g. eventual complexation with organic matter) was not considered because Cs shows poor affinity with dissolved organic matter and remains mainly under its free species $Cs^+$ form. Therefore, $D_{gel}$ was taken equal to the diffusion coefficient of $Cs^+$ in water $D_{water}$. $D_{sed}$ was derived from the coefficient of $Cs^+$ in water corrected to account for the tortuosity during the diffusion in the soil layer, according to the Millington and Quirk's relationship, which states that tortuosity depends on porosity $\varphi$ and water content $\theta$:

(Equation 10) $$D_{sed} = Tortuosity.D_{water} = \frac{\theta^{10/3}}{\varphi^2}.D_{water}$$

Equations at the interface soil-DGT are built according to the same principles presented in Harper et al. (1998).

## 2.5 Calibration of the DGT-PROFS model parameters

In summary, the model is described by five parameters, i.e. the kinetic parameters $k^*_{ads,1}$, $k^*_{des,1}$, $k^*_{ads,2}$ and $k^*_{des,2}$, and the proportion of particulate Cs associated to weak sites $\alpha_{weak}$. Only a few experimental data are available for each experiment (i.e. Cs accumulated on DGT at different times). So additional reasonable assumptions were considered to reduce the number of parameters to be fitted. The first assumption is that the sediment is under equilibrium conditions before the deployment of the DGT device, i.e. $\left[\frac{\partial(MS_{strong})}{\partial t}\right]_{t=0} = 0$. Equation (8) can then be written:

(Equation 11) $$\frac{(MS_{strong})_{t=0}}{(MS_{weak})_{t=0}} = \frac{k^*_{ads,2}}{k^*_{des,2}} = \frac{1-\alpha_{weak}}{\alpha_{weak}}$$

The value of $k^*_{ads,2}$ can then be derived from $k^*_{des,2}$ and $\alpha_{weak}$.

Similarly, it can be assumed that the sediment-water system is at equilibrium and that no diffusion occurs before DGT deployment, i.e. $\frac{\partial(M_{pw,labile})}{\partial t} = 0$. Equation (6) can then be written:

(Equation 12) $$\frac{(MS_{weak})_{t=0}}{(M_{pw,labile})_{t=0}} = \frac{k^*_{ads,1}}{k^*_{des,1}.Sed} = \alpha_{weak}.\frac{(MS_{weak})_{t=0}+(MS_{strong})_{t=0}}{(M_{pw,labile})_{t=0}} = \alpha_{weak}.K_{d,0}$$

where $K_{d,0}$ is the distribution coefficient of Cs between the solid and liquid phase at the beginning of the experiment.

The value of $k^*_{ads,1}$ can then be derived from $k^*_{des,1}$, $\alpha_{weak}$ and from the observed ratio between particulate and dissolved cesium at initial time.

Then, for each soil condition, the DGT-PROFS model allows one to fit the following parameters: $\alpha_{weak}$, the proportion of particulate Cs associated to weak sites; $k^*_{des,1}$, the desorption rate from weak particulate sites; and $k^*_{des,2}$, the desorption rate from strong particulate sites.

These parameters can be obtained by fitting the DGT experimental measurements using a probabilistic approach described in detail in Ciffroy et al. (2011). We remind here the main principles of the calibration approach. A great number of $\{\alpha_{weak}; k^*_{des,1}; k^*_{des,2}\}$ combinations (10000 combinations) were randomly sampled within a large range of potential parameter values (e.g. $\alpha_{weak}$ is randomly sampled from 0 to 1) and the model was run for each of them. For each combination, the error of prediction was calculated as the sum of squared distances between measured and experimental Cs concentrations on DGT. The $\{\alpha_{weak}; k^*_{des,1}; k^*_{des,2}\}$ combinations were then ranked from those given the lowest error to those given the highest one. The top 100 best combinations were selected and weighted for building PDFs for each of the three investigated parameters according to the procedure described in Ciffroy et al (2011). In conclusion, this method allows us to represent parameters by PDFs (i.e., with indications of their uncertainty) instead of single values.

## 3. Results

### 3.1 Cs initial distribution in soils

It is assumed that the Cs depletion induced in the soil porewater for short exposure time occurred on a limited distance from the DGT interface (Harper et al., 2000). Therefore concentration of Cs in the soil porewater extracted by centrifugation at time 4 was considered as not impacted by the presence of DGT and used as a surrogate of the concentration of Cs in the soil porewater at the beginning of the experiments. These concentrations were respectively $4.32 \times 10^{-7} \pm 9.3 \times 10^{-8}$ mol.L$^{-1}$, $3.28 \times 10^{-4} \pm 1 \times 10^{-5}$ mol.L$^{-1}$ and $3.28 \times 10^{-4} \pm 8.5 \times 10^{-6}$ mol.L$^{-1}$ in conditions A, B and C respectively. It corresponds to $0.16 \pm 0.03$ % of total Cs in the soil in condition A, while it represents $1.42 \pm 0.01$ and $1.64 \pm 0.04$ % for conditions B and C respectively showing that most part of Cs was sorbed to the soil particles. Concentration of Cs in soil porewater can be used to calculate the distribution coefficient Kd, defined

as the ratio between Cs concentration sorbed on particles to the Cs concentration in the soil porewater. The values ranged between 282 ± 69, 33 ± 1 and 33 ± 1 $L.kg^{-1}$ for condition A, B and C respectively. Kd for condition A is in accordance with the mean Kd value reported by IAEA (IAEA, 2010) for Cs in silty-clay soils, whereas Kd for condition B and C are slightly lower than the minimal value reported by IAEA (that is 39 $L.kg^{-1}$).

Total concentration of Cs impacted highly the liquid-solid distribution of Cs within this soil, with one order of difference in Kd between condition A and B. Such behaviour relates to the non-linear sorption of Cs as a function of concentration (Missana et al., 2014). Concentrations of Cs used in this study have been chosen based on previous works on the same soil (Cherif, 2017) in order to cover different parts of Cs sorption isotherm. As expected, our Kd values are in agreement with those reported by Cherif (2017). This author conducted 48h contact-time sorption experiments and showed a decrease of Kd from more than 3000 $L.kg^{-1}$ for small concentration of Cs to about 30 $L.kg^{-1}$ for high concentration of Cs. Condition A reproduced conditions of low Cs concentrations just above the inflection point of the sorption isotherm (around $10^{-7}$ $mol.L^{-1}$) whereas condition B reproduced conditions of high Cs concentrations.

Effect of contamination ageing was not evidenced from the solid-liquid distribution of Cs, as seen from the comparison of Kd in condition B and C. Some authors showed that ageing effect was more pronounced in organic than in mineral soils (Rigol et al., 1999b). However while Kd values allow us to measure the capacity of soils to sorb Cs, desorption experiments are necessary to assess the reversibility of Cs adsorption (a low or a high Kd value being not in itself an indicator of the reversibility of sorption or of the absence of kinetically-controlled interactions with soil particles) and highlight potential ageing effect (Gil-Garcia et al., 2008).

Based on previous results of Cherif (2017), where evolution of soil solution chemistry has been measured during sorption/desorption experiments, no modification due to biogeochemical processes (for ex. soil solution chemistry changes induced by soil microbiology) was expected to have impacted our results during the DGT exposure time.

### 3.2 Cs flux to DGT

The measured flux of Cs to the DGT resin over time for the three experimental conditions and their replicates is shown in Figure 2. To facilitate the comparison between the experiments and the replicates, results are normalized to the total amount of Cs in soil (i.e. 'Mean flux of Cs onto DGT' is expressed in mol Cs onto $DGT.h^{-1}.cm^{-2}.mol^{-1}$ of total Cs in soil before DGT implementation). Cs flux on DGT followed similar shapes for all conditions, except for experiment A2 showing a relatively stable

flux over time. They are characterized by a continuous decline of Cs flux onto DGT resin over time, this trend being more significant for conditions B and C. According to the qualitative classification defined by Harper et al. (2000), these conditions can be considered representative of 'diffusive' or 'partial-non-steady state' cases: the DGT device progressively depletes porewater concentrations while the resupply from particles cannot be sustained (in opposition to 'sustained' or 'partial' systems, where the resupply is sufficiently fast so as to maintain a constant flux to DGT over time). This double effect (depletion in porewater not totally sustained by desorption from particles) explains the progressive decrease of accumulation rate on DGT. Nevertheless, even if the shapes were similar, different levels and slopes were observed for conditions A, B and C with flux decreasing from about $7x10^{-5}$ to $4x10^{-5}$ $mol.h^{-1}.cm^{-2}.mol^{-1}$ Cs in soil for condition A, from about $6x10^{-4}$ to $2x10^{-4}$ for condition B and from about $4x10^{-4}$ to $1.5x10^{-4}$ for condition C. In accordance with these fluxes, Cs trapped by DGT after 96h of deployment represented 1.03 ± 0.11% of total Cs in soil in condition A, 4.79 ± 0.28% in condition B and 4.05 ± 0.15% in condition C. Few studies have been devoted up to date to study desorption kinetics of Cs in soils. Liu et al. (2003) observed also a two-step kinetics of Cs desorption from contaminated sediments sampled at Hanford Site. The first stage consisting of a rapid initial release of Cs was followed by a slow kinetic one. Recently Murota et al. (2016) recorded the same pattern of desorption kinetics on natural Japanese soils contaminated by the Fukushima nuclear accident using the "infinite bath" technique of Wauters et al. (1994). In this technique, Cs released in soil solution is immediately captured by a sorbent, which like DGT stimulates desorption by maintaining a virtually "zero" concentration of Cs in soil solution. They found a continuous release of Cs from soils during 139 days, but with desorption fluxes decreasing with time.

Effect of contamination level on yield of desorption and Cs flux to DGT was evidenced by the comparison of condition A and B, with fluxes about one order of magnitude higher in condition with a high level of Cs contamination. An increase in desorption yield with an increase in Cs contamination level was frequently found in literature (Durrant et al., 2018; Tachi et al., 2020).

Effect of ageing was less clear, but a lower flux rate was recorded in condition C compared to condition B, leading to a smaller amount of Cs extracted by DGT upon 96 hours. While less release of Cs following increased contact time with Cs contamination has been reported by several authors on soils (Valcke and Cremers, 1994; Roig et al., 2007; Al Attar et al., 2016; Murota et al., 2016), or sediments (Ciffroy et al., 2001), others failed to demonstrate it (Zachara et al., 2002). As stated previously, impact of ageing may depend on soil nature and particularly on the content of organic matter (Rigol et al., 1999a; Roig et al., 2007).

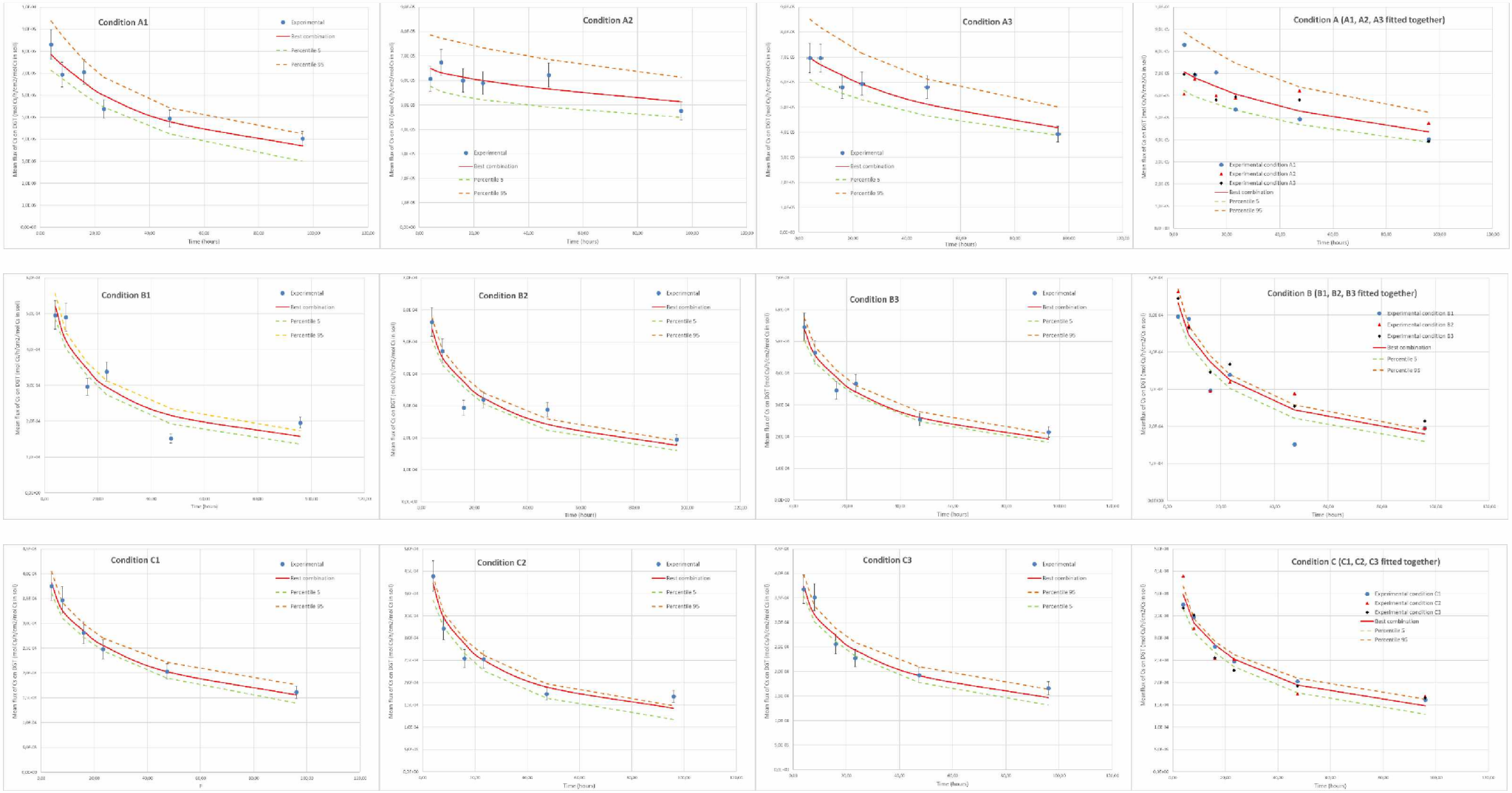


537 **Figure 2** – Mean flux of Cs onto DGT (in mol $Cs.d^{-1}.cm^{-2}.mol^{-1}$ Cs in soil). The points represent experiment data – The continuous line represents the curve

538 obtained with the best combination of parameter values - The upper and lower dotted lines represent the $5^{th}$ and $95^{th}$ percentiles, respectively

539 Decreases in fluxes with time, as well as difference in fluxes induced by Cs contamination level and
540 ageing, probably result from different distribution of Cs on soil solid particles, with the involvement of
541 multiple sites with different binding affinities for Cs. The objective of the modelling work described
542 below is to quantify these differences, assuming the existence of two kind of binding sites (weak and
543 strong sites), as well as the kinetic desorption rates associated to these sites.

544

545 **3.3 Modeling results and interpretation of parameter values**

546 The model previously described was calibrated for each of the experiments, i.e. for the three replicates
547 of each condition, as well as for each condition A, B and C considering all replicates together. For any
548 deployment time of the DGT, the comparison between model and experimental flux onto DGT is
549 reported in Figure 2. The continuous line in Figure 2 represents the calculated flux kinetics obtained
550 with the best combination of parameter values, while the upper and lower dotted lines represent the
551 5$^{th}$ and 95$^{th}$ percentiles, respectively. Results demonstrate that the average curve generally agrees well
552 with experimental data and that the area encompassed by the 5$^{th}$ and the 95$^{th}$ percentiles includes
553 experimental data points (except for experimental outliers like in experiment B1 and B2).

554 Fitted parameter values, i.e. the values of the desorption kinetic rates $k^*_{des,1}$ and $k^*_{des,2}$, as well as the
555 proportion of Cs adsorbed onto the weak sites $\alpha_{weak}$, are reported in Table 2. First, it can be noted
556 that the standard deviations calculated for the normal PDFs reported in Table 2 are generally low. That
557 means that the top 100 best $\{\alpha_{weak}; k^*_{des,1}; k^*_{des,2}\}$ combinations identified in the calibration
558 procedure are quite homogeneous. The range of simulated parameter values is thus generally tight
559 revealing that the uncertainty in the prediction is low. Variability on $k^*_{des,1}$ and $k^*_{des,2}$ between
560 replicates for a given condition is also very limited, except in condition A were experiment A2 showed
561 a specific pattern.

562 Experimental conditions did not show any major impact on desorption rates, $k^*_{des,1}$ and $k^*_{des,2}$, which
563 remained generally on similar orders of magnitude: when considering mean values of the calculated
564 PDFs (Table 2) (excepting experiment A2), $k^*_{des,1}$ ranges between 9.4x10$^{-6}$ (condition A3) and 5x10$^{-5}$
565 (condition B1) s$^{-1}$ and $k^*_{des,2}$ ranges from 4.8x10$^{-8}$ to 5x10$^{-8}$ s$^{-1}$ (Table 2). A slight effect of contamination
566 level may appear on $k^*_{des,1}$ with lower values of desorption from the weak sites at low Cs
567 concentration. However due to the high dispersion of data in condition A, this findings must be taken
568 cautiously. Desorption rate constants from the stronger site are not affected by contamination level
569 and ageing. Desorption rate constant is conceptually an intrinsic property of the site involved in
570 sorption. Thus as long as these sites remain the same between our conditions, no change in $k^*_{des,1}$ or

571 $k^*_{des,2}$ was expected. However involvement of different sorption sites depending on the tested
572 conditions would have resulted in different $k^*_{des,1}$ or $k^*_{des,2}$. Sorption of Cs at high concentration could
573 have involved exchangeable sites non-solicited at lower Cs concentration. This assumption cannot be
574 ruled out by comparing values of $k^*_{des,1}$ between condition A and B.

575 **Table 2** - Calculated parameters with the DGT-PROFS model for the different conditions tested
576 $\mathcal{N}(\mu\ ;\ \sigma)$ is the normal distribution with the mean $\mu$ and the standard distribution $\sigma$

| Condition | Ratio between Cs associated to weak sites to total particulate Cs: $\alpha_{weak}$ (-) | $k^*_{des,1}$ ($s^{-1}$) Desorption rate from weak sites: | $k^*_{des,2}$ ($s^{-1}$) Desorption rate from strong sites: |
|---|---|---|---|
| A1 | $\mathcal{N}(0.14\ ;\ 0.024)$ | $\mathcal{N}(3.1.10^{-5}\ ;\ 1.1.10^{-5})$ | $\mathcal{N}(5.10^{-8}\ ;\ 2.5.10^{-8})$ |
| A2 | $\mathcal{N}(0.49\ ;\ 0.1)$ | $\mathcal{N}(2.6.10^{-6}\ ;\ 6.6.10^{-7})$ | $\mathcal{N}(5.10^{-8}\ ;\ 2.5.10^{-8})$ |
| A3 | $\mathcal{N}(0.22\ ;\ 0.04)$ | $\mathcal{N}(9.4.10^{-6}\ ;\ 3.10^{-6})$ | $\mathcal{N}(4.9.10^{-8}\ ;\ 2.4.10^{-8})$ |
| *A (A1, A2 and A3 fitted together)* | *$\mathcal{N}(0.23\ ;\ 0.05)$* | *$\mathcal{N}(9.9.10^{-6}\ ;\ 3.2.10^{-6})$* | *$\mathcal{N}(4.9.10^{-8}\ ;\ 2.5.10^{-8})$* |
| B1 | $\mathcal{N}(0.29\ ;\ 0.023)$ | $\mathcal{N}(5.10^{-5}\ ;\ 1.10^{-5})$ | $\mathcal{N}(5.10^{-8}\ ;\ 2.5.10^{-8})$ |
| B2 | $\mathcal{N}(0.36\ ;\ 0.03)$ | $\mathcal{N}(4.1.10^{-5}\ ;\ 7.9.10^{-6})$ | $\mathcal{N}(4.9.10^{-8}\ ;\ 2.5.10^{-8})$ |
| B3 | $\mathcal{N}(0.40\ ;\ 0.03)$ | $\mathcal{N}(3.2.10^{-5}\ ;\ 5.7.10^{-6})$ | $\mathcal{N}(4.9.10^{-8}\ ;\ 2.4.10^{-8})$ |
| *B (B1, B2 and B3 fitted together)* | *$\mathcal{N}(0.35\ ;\ 0.03)$* | *$\mathcal{N}(3.9.10^{-5}\ ;\ 7.7.10^{-6})$* | *$\mathcal{N}(4.9.10^{-8}\ ;\ 2.5.10^{-8})$* |
| C1 | $\mathcal{N}(0.24\ ;\ 0.04)$ | $\mathcal{N}(1.55.10^{-5}\ ;\ 4.6.10^{-6})$ | $\mathcal{N}(4.8.10^{-8}\ ;\ 2.4.10^{-8})$ |
| C2 | $\mathcal{N}(0.17\ ;\ 0.02)$ | $\mathcal{N}(3.2.10^{-5}\ ;\ 9.10^{-6})$ | $\mathcal{N}(4.9.10^{-8}\ ;\ 2.4.10^{-8})$ |
| C3 | $\mathcal{N}(0.19\ ;\ 0.03)$ | $\mathcal{N}(1.63.10^{-5}\ ;\ 4.8.10^{-6})$ | $\mathcal{N}(5.10^{-8}\ ;\ 2.5.10^{-8})$ |
| *C (C1, C2 and C3 fitted together)* | *$\mathcal{N}(0.20\ ;\ 0.03)$* | *$\mathcal{N}(2.10^{-5}\ ;\ 6.10^{-6})$* | *$\mathcal{N}(5.10^{-8}\ ;\ 2.5.10^{-8})$* |

577

578 Comparing desorption rates to already published data is difficult due to the small number of studies
579 devoted to Cs desorption kinetics in natural soils. Most studies that have considered chemical kinetic
580 reactions for sorption/desorption of Cs in soils or sediments have proposed models based on two sites,
581 with one site at equilibrium with the porewater and one site involving either a kinetics of sorption and
582 no desorption (meaning Cs is irreversibly fixed on this second site) or kinetics for both sorption and
583 desorption, like in this study. Thus few authors have considered the existence of kinetic reactions on

584 two sites. Murota et al. (2016) have assumed the existence of three successive sites with Cs desorption
585 following a pseudo first-order reaction kinetics from all of them. They used their models to describe
586 results of Cs desorption from Japanese soils, contaminated with $^{137}Cs$ following the Fukushima-Daïchi
587 nuclear power plant accident, acquired through the "infinite bath" technique (Wauters et al., 1994),
588 which make them particularly relevant to be compared to our results acquired with DGT. The average
589 desorption rates for their three sites are $1x10^{-8}$, $7x10^{-7}$, and $4.5x10^{-6}$ $s^{-1}$, from the stronger to the weaker
590 sites respectively. Absalom et al. (1996) studied the dynamics of $^{137}Cs$ sorption/desorption in artificially
591 contaminated organic and mineral soils, with a three box model. They reported a kinetic rate of
592 desorption from "strong-like" sites of $1.7x10^{-8}$ $s^{-1}$ in a mineral soil, while it was one order of magnitude
593 higher for organic soils. In our study, $k^*_{des,2}$ values are in good agreement with desorption rate
594 constants reported for strong sites by Murota et al. (2016) and Absalom et al. (1996) on soils. They fell
595 also within the range of desorption rate constant reported from natural sediments ($1.2x10^{-8}$ $s^{-1}$) by Liu
596 et al. (2003). These slow desorption rates is assumed to be a consequence of the diffusion of Cs within
597 interlayer of illite or other micaceous minerals (Murota et al., 2016, Okumura et al., 2018). As said
598 previously, comparing $k^*_{des,1}$ to published data is difficult since in most multi-sites models, the first site
599 is supposed to be an exchangeable site in equilibrium with soil porewater; exhibiting therefore no
600 kinetic limitation. However our values of $k^*_{des,1}$ encompass the desorption rate constant proposed by
601 Murota et al. (2016) for their weaker site as previously mentioned.

602 Effect of contamination level or ageing was expected on the distribution of Cs among weak and strong
603 sites. Significant differences were indeed obtained on the fraction of Cs associated to weak sites,
604 $\alpha_{weak}$. Higher $\alpha_{weak}$ values were obtained for condition B (mean values: 29 to 40 %; 35% when all
605 replicates are calibrated together, with a 90% confidence interval ranging from 29 to 41%), while only
606 a small fraction of Cs is associated to weak sites under condition A1 and A3 (14 and 22% respectively;
607 23% when all replicates are calibrated together, with a 90% confidence interval ranging from 13 to
608 32%). All these results should be taken with caution since parameter values show variability among
609 replicates, especially in condition A where the concentration of Cs was low. Such a variability may be
610 explained by the fact that DGT accumulation is influenced by local conditions at the interface between
611 the DGT membrane and soil and that a greater number of replicates would be necessary to improve
612 the robustness of the evaluation. But it could also relate to the very small quantity of Cs recovered by
613 DGT in condition A and the higher analytical uncertainty in this condition. Anyway the increase in
614 $\alpha_{weak}$ with increasing Cs contamination can be explained by saturation of sorption sites on clay
615 particles. Indeed, FES sites, which are the sites with the strongest Cs affinity, are also the smaller in
616 terms of density. Therefore, when the contamination level is too high (conditions B and C), FES sites
617 are saturated, leading to a redistribution of Cs among sorption sites present at the planar surface,

surface of frayed edge sites and/or strong interlayer (Missana et al., 2014; Cherif, 2017). With ageing, Cs is supposed to move into core region of illite particles. Therefore a decrease of $\alpha_{weak}$ was expected. While simple graphical analysis of results did not put in evidence ageing effect, modelling results indicate that the $\alpha_{weak}$ slightly decreased between conditions B and C from 35% (90% confidence interval [0.29-0.41]) to 20% (90% confidence interval [0.14-0.26]) when all replicates are calibrated together).

## 4. Conclusion

Predicting the dynamics of Cs at the particle/porewater interface in soils is an important task since this interaction partly controls its subsequent bioavailability to plants or soil organisms, but also migration to deeper soil horizons. A kinetic DGT experimental approach combined to the interpretation with the DGT-PROFS model was able to predict Cs dynamics at the particle-porewater interface of soils under various conditions. It was shown that the resupply of Cs to porewater from soil solid phases was modified according to contamination level, and that a slight ageing effect was put in evidence. The DGT-PROFS model showed that desorption kinetic rates were not significantly modified by contamination level and ageing. Cs partitioning between weak and strong adsorption sites was instead influenced by the contamination level, suggesting saturation effects. These results acquired on one soil should be further confirmed by studying soils with different properties. Content of clays and organic matter, but also nature of clay minerals, are known to be the main parameters controlling Cs sorption/desorption in soils. However this study demonstrates the suitability of DGT combined with a multi-compartmental model to extract parameters describing Cs desorption dynamic in soils. Such parameters can be further used in radioecological transfer model to predict Cs mobility or assess Cs impact in terrestrial ecosystem.

## Acknowledgments

The authors would like to thank the French NEEDS-Environment program for funding the TECHMO-3D (Modélisation Dynamique de la Disponibilité du césium dans le sol : interprétation des flux de Cs à l'aide de mesures DGT) project.

## References


Absalom J.P., Crout N.M.J., Young S.D., 1996. Modeling radiocesium fixation in upland organic soils of Northwest England. Environ. Sci. Technol. 30, 2735–2741

Al Attar L., Al-Oudat M., Safia B., Ghani B.A. 2016. Ageing impact on the transfer factor of $^{137}$Cs and $^{90}$Sr to lettuce and winter wheat. J. Environ. Radioact. 164: 19-25

Balonov M.I., Bruk G.Y., Golikov V.Y., Barkovsky A.N., Kravtsova E.M., Kravtosova O.S., Mubasarov A.A., Shutov V.N., Travnikova I.G., Howard B.J., Brown J.E., Strand P. 2007. Assessment of current exposure of the population living in the Techa river basin from radioactive releases of the Mayak facility. Health Physics 92: 134-147

Beresford N.A., Fesenko S., Konoplev A., Skuterud L., Smith J.T., Voigt G. 2016. Thirty years after the Chernobyl accident: What lessons have we learnt? J. Environ. Radioact. 157: 77-89

Bradbury M.H. and Baeyens B. 2000. A generalised sorption model for the concentration dependent uptake of caesium by argillaceous rocks. J. Cont. Hydrol. 42: 141-163

Brimo K., Gonze M-A., Pourcelot L. 2019. Long term decrease of $^{137}$Cs bioavailability in French pastures: Results from 25 years of monitoring. J. Environ. Radioact. 208–209: 106029

Brouwer E., Baeyens B., Maes A., Cremers A. 1983. Cesium and rubidium ion equilibrium on illite clays. The Journal of Physical Chemistry 87: 1213-1219

Chaif H., Coppin F., Bahi A., Garcia-Sanchez L. 2021. Influence of non-equilibrium sorption on the vertical migration of $^{137}$Cs in forest mineral soils of Fukushima prefecture. J. Environ. Radioact. 232: 106567

Chang L.-Y., Davison W., Zhang H., Kelly M. 1998. Document Performance characteristics for the measurement of Cs and Sr by diffusive gradients in thin films (DGT). Anal. Chim. Acta 368: 243-253

Cherif M.A. 2017. Modélisation dynamique de la (bio)disponibilité des radionucléides dans les sols : approche comparative modèles-expériences appliquée au transfert de césium dans la rhizosphère. PhD thesis. Aix-Marseille University

Cherif M.A., Martin-Garin A., Gérard F., Bildstein O. 2017. A robust and parsimonious model for caesium sorption on clay minerals and natural clay materials. Appl. Geochem. 87: 22-37

Ciffroy P., Garnier J-M., Pham M. K. 2001. Kinetics of the adsorption and desorption of radionuclides of Co, Mn, Cs, Fe, Ag and Cd in freshwater systems: experimental and modelling approaches. J. Environ. Radioact. 55: 71-91

Ciffroy P., Garnier J-M., Benyahya L. 2003. Kinetic partitioning of Co, Mn, Cs, Fe, Ag, Zn and Cd in fresh waters (Loire) mixed with brackish waters (Loire estuary): experimental and modelling approaches. Mar. Pollut. Bulletin 46: 626-641

Ciffroy P., Nia Y., Garnier J-M. 2011. Probabilistic multicompartmental model for interpreting DGT kinetics in sediments. Environ. Sci. Technol. 45: 9558-9565

Comans R., Hockley D. 1992. Kinetics of cesium sorption on illite. Geochim. Cosmochim. Acta, 56, 1157–1164

Comans R.N., Haller M., De Preter P. 1991. Sorption of cesium on illite: non-equilibrium behaviour and reversibility. Geochim. Cosmochim. Acta *55*(2), 433-440

Cornu J-Y., Denaix L., Schneider A., Pellerin S. 2007. Temporal evolution of redox processes and free Cd dynamics in a metal contaminated soil after rewetting. Chemosphere, 70, 306–314

Cremers A., Elsen A., De Preter P., Maes A. 1988. Quantitative analysis of radiocaesium retention in soils. Nature 335: 247–249

Davison W., Zhang H. 1994. In situ speciation measurements of trace components in natural waters using thin-film gels. Nature 367: 546-548

De Koning A., Comans R.N. 2004. Reversibility of radiocaesium sorption on illite. Geochim. Cosmochim. Acta 68 (13), 2815–2823.

Devau N., Le Cadre E., Hinsinger P., Gérard F. 2011. Fertilization and pH effects on processes and mechanisms controlling dissolved inorganic phosphorus in soils. Geochim. Cosmochim. Acta 75: 2980-2996

Durrant C.B., Begg J.D., Kersting A.B., Zavarin M. 2018. Cesium sorption reversibility and kinetics on illite, montmorillonite and kaolinite. Sci. Total Environ. 610-611: 511–520

Ernstberger H., Davison W., Zhang H., Tye A., Young S. 2002. Measurement and Dynamic Modeling of Trace Metal Mobilization in Soils Using DGT and DIFS. Environ. Sci. Technol. 36: 349–354

Evans C.H., Alberts J.J., Clark R.A. 1983. Reversible ion-exchange fixation of Cs-137 leading to mobilisation from reservoir sediments. Geochim. Cosmochim. Acta 47: 1041–1049

Fuller A.J., Shaw S., Peacock C.L., Trivedi D., Small J.S., Abrahamsen L.G., Burke I.T. 2014. Ionic strength and pH dependent multi-site sorption of Cs onto a micaceous aquifer sediment Applied Geochem. 40: 32-42

Fuller A.J., Shaw S., Ward M.B., Haigh S.J., Mosselmans F.W., Peacock C.L., Stackhouse S., Dent A.J., Trivedi D., Burke I.T. 2015. Caesium incorporation and retention in illite interlayers. Appl. Clay Sci. 108: 128–134

Garnier J-M., Ciffroy P., Benyahya L. 2006. Implications of short and long term (30 days) sorption on the desorption kinetic of trace metals (Cd, Zn, Co, Mn, Fe, Ag, Cs) associated with river suspended matter. Sci. Tot. Environ. 366: 350-360

Gil-Garcia C.J., Rigol A., Rauret G., Vidal M. 2008. Radionuclide sorption–desorption pattern in soils from Spain. Appl. Rad. Isot. 66: 126–138

Gorny J., Gourgiotis A., Coppin F., Février L., Zhang H., Simonucci C. 2019. Better understanding and applications of ammonium 12-molybdophosphate-based diffusive gradient in thin film techniques for measuring Cs in waters. Environ. Sci. Pollut. Res. 26: 1994-2006

Harper M.P., Davison W., Zhang H., Tych W. 1998. Kinetics of metal exchange between solids and solutions in sediments and soils interpreted from DGT measured fluxes. Geochim. Cosmochim. Acta 62: 2757–2770

Harper M.P., Davison W., Tych W. 2000. DIFS - A modelling and simulation tool for DGT induced trace metal remobilisation in sediments and soils. Environ. Model. Software 15: 55-66

IAEA (International Atomic Energy Agency). 2010. Handbook of Parameter Values for the Prediction of Radionuclide Transfer in Terrestrial and Freshwater Environments. 978-92-0-113009-9 Technical Reports Series No. 472

Kasar S., Mishra S., Omori Y., Sahoo S.K., Kavasi N., Arae H., Sorimachi A., Aono T. 2020 Sorption and desorption studies of Cs and Sr in contaminated soil samples around Fukushima Daiichi Nuclear Power Plant. J. Soils Sediments 20: 392–403

Lehto N.J., DavisonW., Tych W., Zhang H. 2008. Quantitative assessment of soil parameter (KD and TC) estimation using DGT measurements and the 2D DIFS model. Chemosphere, 71, 795–801

Li W., Wang F., Zhang W., Evans D. 2009. Measurement of stable and radioactive cesium in natural waters by the diffusive gradients in thin films technique with new selective binding phases. Anal. Chem. 81: 5889-5895

Liu C., Zachara J.M., Smith S.C., Mc Kinley J.P., Ainsworth C.C. 2003. Desorption kinetics of radiocesium from subsurface sediments at Hanford Site, USA. Geochim. Cosmochim. Acta 67: 2893–2912

Mihalík J., Henner P., Frelon S., Camilleri V., Fevrier L. 2012. Citrate assisted phytoextraction of uranium by sunflowers: study of fluxes in soils and plants and resulting intra-planta distribution of Fe and U. Environ. Exp. Bot. 77: 249-258

Missana T., García-Gutiérrez M., Benedicto A., Ayora C., De-Pourcq K. 2014. Modeling of Cs sorption in natural mixed-clays and the effects of ion competition. Appl. Geochem. 49: 95-102.

Murdock C., Kelly M., Chang L.-Y., Davison W., Zhang H. 2001. DGT as an in situ tool for measuring radiocesium in natural waters. Environ. Sci. Technol. 35: 4530-4535

Murota K., Saito T., Tanaka S. 2016. Desorption kinetics of cesium from Fukushima soils. J. Environ. Radioact. 153: 134-140

Nia Y., Garnier J-M., Rigaud S., Hanna K., Ciffroy P. 2011 Mobility of Cd and Cu in formulated sediments coated with iron hydroxides and/or humic acids: a DGT and DGT-PROFS modeling approach. Chemosphere. 85: 1496-1504

Nowack B., Koehler S., Schulin R. 2004. Use of Diffusive Gradients in Thin Films (DGT) in undisturbed field soils. Environ. Sci. Technol. 38: 1133–1138

Okumura M., Kerisit S., Bourg I.C., Lammers L.N., Ikeda T., Sassi M., Rosso K.M., Machida M. 2018 Radiocesium interaction with clay minerals: Theory and simulation advances Post–Fukushima. J. Environ. Radioact. 189: 135-145

Poinssot C., Baeyens B., Bradbury M.H. 1999. Experimental and modelling studies of caesium sorption on illite. Geochim. Cosmochim. Acta 63: 3217-3227

Rigol A., Vidal M., Rauret G. 1999a. Effect of the ionic status and drying on radiocesium adsorption and desorption in organic soils. Environ. Sci. Technol. 33: 3788-3794

Rigol A., Roig M., Vidal M., Rauret G. 1999b. Sequential extractions for the study of radiocesium and radiostrontium dynamics in mineral and organic soils from Western Europe and Chernobyl areas. Environ. Sci. Technol. 33: 887-895

Rigol A., Vidal M., Rauret G. 2002. An overview of the effect of organic matter on soil-radiocaesium interaction: Implications in root uptake Journal of Environmental Radioactivity 58: 191-216

Roig M., Vidal M., Rauret G., Rigol A. 2007. Prediction of Radionuclide Aging in Soils from the Chernobyl and Mediterranean Areas. J. Environ. Qual. 36: 943–952

Siroux B., Wissocq A., Beaucaire C., Latrille C., Petcut C., Calvaire J., Tabarant M., Benedetti M.F., Reiller P.E. 2018. Adsorption of strontium and caesium onto an Na-illite and Na-illite/Na-smectite mixtures: Implementation and application of a multi-site ion-exchange model. Appl. Geochem. 99: 65-74

Sochaczewski Ł., Tych W., Davison B., Zhang H. 2007. 2D DGT induced fluxes in sediments and soils (2D DIFS). Environ. Model. Software 22: 14-23

Steinhauser G., Niisoe T., Harada K.H., Shozugawa K., Schneider S., Synal H-A., Walther C., Christl M., Nanba K., Ishikawa H., Koizumi A. 2015. Post-accident sporadic releases of airborne radionuclides from the Fukushima Daiichi nuclear power plant site. Environ. Sci. Technol. 49: 14028-14035

Tachi Y., Sato T., Takeda C., Ishidera T., Fujiwara K., Iijima K. 2020. Key factors controlling radiocesium sorption and fixation in river sediments around the Fukushima Daiichi Nuclear Power Plant. Part 2: Sorption and fixation behaviors and their relationship to sediment properties Sci. Tot. Environ. 724: 138097

Valcke E., Cremers A. 1994. Sorption-desorption dynamics of radiocaesium in organic matter soils. Sci. Tot. Environ. 157: 275-283

Wauters J., Sweeck L., Valcke E., Elsen A., Cremers A. 1994. Availability of radiocaesium in soils: a new methodology. Sci. Tot. Environ. 157: 239-248

Wissocq A., Beaucaire C., Latrille C. 2018. Application of the multi-site ion exchanger model to the sorption of Sr and Cs on natural clayey sandstone. Appl. Geochem. 93: 167-177

Zachara J.M., Smith S.C., Liu C., McKinley J.P., Serne R.J., Gassman P.L. 2002. Sorption of Csþ to micaceous subsurface sediments from the Hanford site, USA. Geochem. Cosmochim. Acta 66: 193–211

Zhang H., Davison W., Knight B., McGrath S. 1998. In situ measurements of solution concentrations and fluxes of trace metals in soils using DGT. Environ Sci Technol. 32: 704–710